Research Square

Preprints are preliminary reports that have not undergone peer review.
They should not be considered conclusive, used to inform clinical practice,
or referenced by the media as validated information.

The Effect of Engine Vibration on Wing Resonance in Boxer Engine UAV Aircraft

Gurkan Ortamevzi

gurkan.ortamevzi@alanya.edu.tr

Alanya Alaaddin Keykubat University

Article

Keywords: wing resonance, boxer engine vibrations, finite element method, modal analysis, short-winged aircraft

Posted Date: May 14th, 2026

DOI: https://doi.org/10.21203/rs.3.rs-9497820/v1

License: This work is licensed under a Creative Commons Attribution 4.0 International License.
Read Full License

Additional Declarations: No competing interests reported.

The Effect of Engine Vibration on Wing Resonance in Boxer Engine UAV Aircraft

Gurkan Ortamevzi

Gazipasa Aerospace Sciences Faculty, Alanya Alaaddin Keykubat University, Antalya, Turkey
*Correspondence: gurkan.ortamevzi@alanya.edu.tr

ABSTRACT

This study investigates the effect of vibrations generated by a short-wing, boxer-engine UAV (unmanned aerial vehicle) on the aircraft's wings. The negative impacts on flight safety caused by wing resonance problems are supported by previously reported aircraft accidents. The frequencies of the dominant vibrations generated by the Rotax-912 boxer engine, frequently used in short-wing UAVs and ultralight aircraft, particularly during climb, cruise, and descent phases, were determined. Mathematical mesh models were created for six different wing models, varying according to rib count and the position of the lateral strut under the wing. The natural frequency values of the wing models were determined using the finite element method and modal analysis for four different mode shapes. These values were compared with the vibration frequency values generated by the engine to interpret the wing's tendency to resonate. The suitability of each wing model for this vibration condition was discussed. Furthermore, to predict the risks that may arise in case of wing resonance, wingtip deformation and von-Misses stress values at different mode frequencies were determined and compared according to model types. This study is useful for UAV or ultralight designers whose aircraft are small enough to be transported in standard containers, as it helps them predict the effects that vibrations can have on the wings.

Keywords

wing resonance; boxer engine vibrations; finite element method; modal analysis; short-winged aircraft

Introduction

When designing aircraft wings, wing strength is the most important parameter. The most significant factor affecting strength is the lift force supporting the aircraft's weight. Generally, stresses resulting from lift can be predicted, and wing structural elements are designed to tolerate these stresses. A more complex and critical factor to predict is vibration. Especially in aircraft with internal combustion engines and propellers, vibrations occur over a very wide frequency range. The amplitudes of these vibrations are quite large. If the frequencies of the vibration generators coincide with the natural frequency of the wings, the vibration amplitude increases exponentially. This is called resonance, and high stresses can be observed in the wing structural elements. Consequently, the fatigue life of the wing structural elements also decreases. Cracks or ruptures can occur in the wing structural elements, especially at the connection points. Numerous fatal aircraft accidents have been reported in relation to this situation. For example, the official accident report states that in Braniff Airways Flight 542, a Lockheed L-188 Electra, vibrations from the engine were transmitted to the wing structure via the engine coupling, and the left wing detached during flight as a result of the vibration frequency coinciding with the wing's natural frequency modes [6]. Similarly, in Northwest Airlines Flight 710, a Lockheed L-188C Electra, the right wing detached due to engine and propeller vibration [5]. The fact that both accidents involved the same model aircraft raises suspicions that the frequency conflict was design related. The detachment of the engine coupling in United Parcel Service (UPS) flight 2976, a McDonnell Douglas MD-11F, was also reported to have occurred due to vibration induced fatigue [19]. These accidents demonstrate that avoiding resonance during the

design phase is crucial for flight safety. First, the frequency bands of vibration sources must be meticulously identified, and then, the natural frequencies of structural elements that could threaten the safe flight of the aircraft should be designed so that they differ sufficiently from the frequency bands of the vibration sources [7,18,24]. Minimizing the transmission of vibrations to the aircraft structural elements reduces the vibration band amplitude. Vibration isolation structures used in the aircraft engine mounting system dampen vibrations, especially those caused by ignition within the engine [21]. The wings of aircraft with short wingspans, especially those using boxer engines, frequently enter these resonance regions [10]. Since ultralight and UAV manufacturers generally deliver aircraft to customers in containers, the wingspan of the aircraft is designed according to the dimensions of standard containers [8].

In this article, the position and number optimization of wing structural elements of an experimental unmanned aerial vehicle with a Rotax-912 engine is performed according to the engine and propeller vibration frequencies. In the Materials and Methods section, the vibrations of the Rotax-912 engine during climb, level flight, and descent are determined. 3D models of the aircraft's left wing, with a wingspan of two meters, were created in different combinations. The reason for choosing a two-meter wingspan is its sensitivity to the dominant frequencies generated in this engine [3,15]. Mathematical mesh models were created from the generated 3D models using the finite element method to determine the natural frequency modes [22]. Each wing structure combination with determined natural frequency modes was discussed in the results and discussion section in terms of frequency mode overlap, deformation, and stress distribution. The effects of a lateral strut that could be added between the wing and the fuselage were also observed.

Materials and Methods

Theory

Aircraft wings, exposed to external factors such as engine vibrations and vibrations caused by the rotational effect of the propeller, are affected by vibration because they are flexible. The tendency of the wing to vibrate at certain frequencies in relation to only its rigidity and mass is called the natural frequency, and the change in shape created by the vibration in the wing at certain frequencies is called the mode shape. The general vibration equation is explained in equation 1 [9].

$$M\,\ddot{q}(t) + K\,q(t) = 0 \tag{1}$$

Here, M is the mass, K is the rigidity, and q is the displacement vector. The equation used to obtain natural frequencies is explained in equation 2 [9].

$$(K - \omega^2 M)\phi = 0 \tag{2}$$

Here, K is the rigidity, ω^2 is the angular natural frequency, M is the mass, and ϕ is the vector of the mode shape.

Vibration modes that can cause structural damage in aircraft wings are the bending mode, which is formed by the up and down flexing of the wing, the torsion mode, which is formed by the periodic rotational movement around the spanwise axis of the wing, and the modes formed by the combination of these movements [12]. In this study, other aeroelasticity problems such as flutter, divergence, and buffeting were ignored in the wing examined, and only the situations related to natural frequency overlaps caused by the effects of engine and propeller vibration were analyzed. The complexity of the wing structure and the number and position optimization of the structural elements to be used in the wing design necessitated the analysis of this study with the finite element method [16,24]. Thanks to

modal analysis, it will be possible to determine the vibration modes that can cause structural damage in advance and to design the wing in a way that will avoid these frequencies.

Vibration sources

In this aircraft, which will use a Rotax 912 engine, engine generated vibrations have been evaluated as force vibrations. The engine's structural feature is its four-cylinder, four-stroke design. However, a gearbox is located between the engine shaft and the propeller shaft. Therefore, the engine speed and propeller speed are different. The engine's climb and cruise speeds are 4800-5500 rpm, while the propeller speed is around 1975-2263 rpm for cruise control [4,20]. This engine is a multi-frequency and multi-source vibration generator. The vibration sources in this engine can be examined in three categories: combustion-related vibrations, mass inertia-related vibrations, and propeller-related vibrations due to reduction, all producing vibrations at different frequencies. Dominant frequency ranges have been evaluated according to the engine's long-term speed ranges. Dominant frequencies are those where the frequencies of combustion-related, inertia-related, and propeller-related vibrations are likely to overlap. The engine's long-term speed ranges are predicted as 5200-5500 rpm for climbing, 4800-5200 rpm for cruising, and 4000-4500 rpm for approach. In this context, the dominant vibration frequencies are calculated as 173-183 Hz for climbing, 160-173 Hz for cruising, and 133-150 Hz for approach [25] The point to be considered in this calculation is that in a four-stroke, four-cylinder engine, each cylinder fires once every two crankshaft revolutions. Therefore, the strongest driving frequency is the second engine order. That is, the dominant frequency, the combustion frequency, is calculated as in equation 3 [23]

$$f_{\text{dom}} = \frac{N_{\text{rpm}}}{60} \times 2 \tag{3}$$

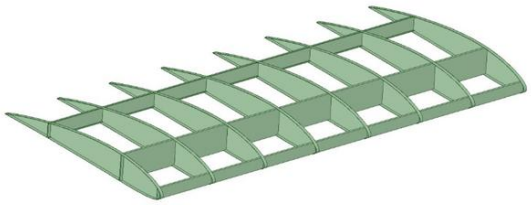
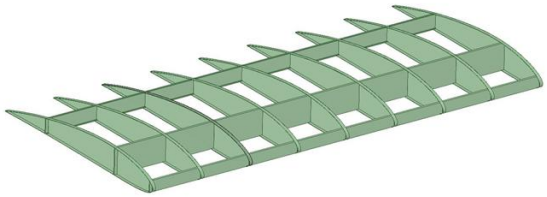
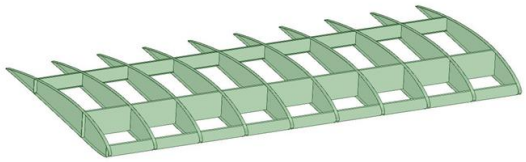
Here, f_{dom} is the dominant frequency, N_{rpm} is the engine speed.

The reason why the strongest dominant frequency is not the first engine order is that the Rotax-912 engine is a boxer type engine. In boxer engines, cylinders working in opposite directions will cancel each other's inertial forces [2]. Propeller-induced vibrations were not included in this study. The propeller speed is lower than the engine speed in Rotax 912, the reduction system in this engine has a damping clutch system and dampens torsional vibrations [13]. However, the vibration isolators used in the engine assembly dampen low-frequency vibrations well [17,21]. In addition, it was assumed in this study that the propeller assembly was done ideally without producing dynamic balance.

3D and mathematical model

Modal analyses of different wing designs were performed using the finite element method to keep the wing's natural frequency modes away from the predicted vibration source frequencies. To perform these analyses, 3D models of possible wing designs were created, and mathematical mesh models of the wing were generated from these 3D models. The 3D model of the left wing with a 2-meter wingspan was created in three variations: 8-rib, 9-rib, and 10-rib. These wing models, showing their internal structure, are presented in Table 1.

Table 1. 3D Models of Wing Type Variations with Name of Wing Type Variation.

	8 rib
	9 rib
	10 rib

To perform modal analysis of the wing variations for which 3D models were created, separate mathematical mesh models were constructed for each model. Additionally, modal analyses were generated using ANSYS Workbench software. The mathematical mesh model of the 9-rib wing variation is shown in Figure 1.

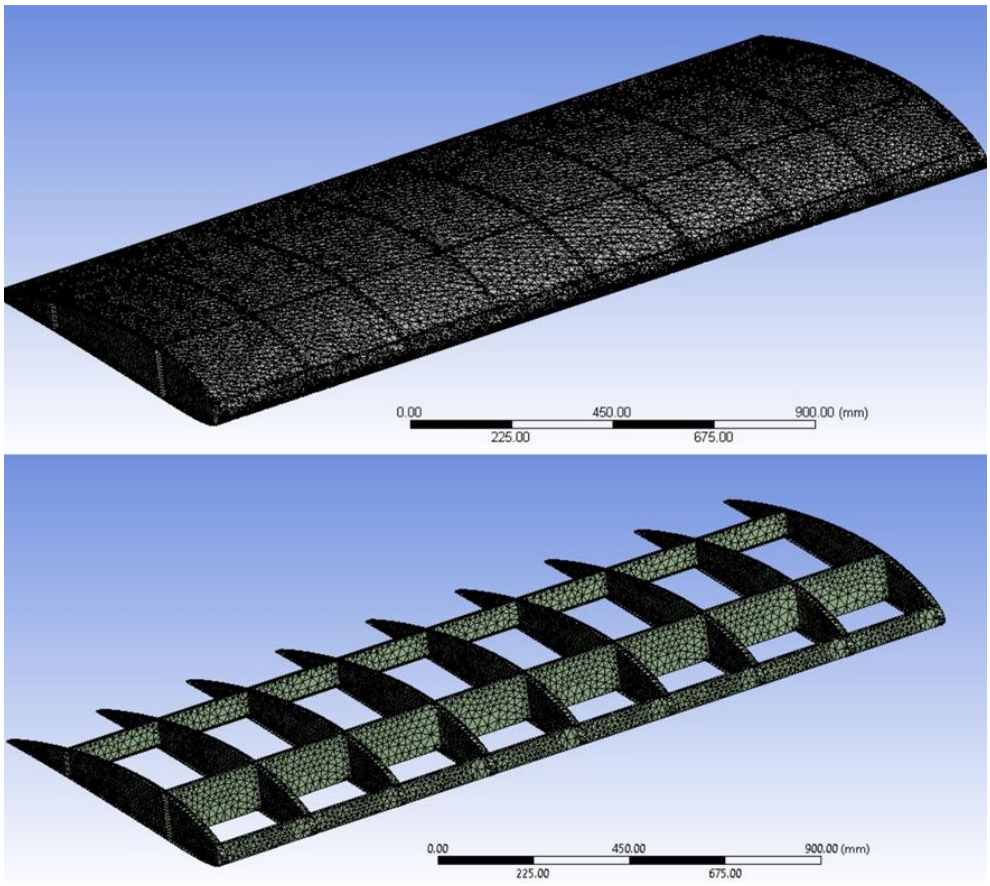


Figure 1. Mathematical mesh model of 9 rib wing type.

In these mathematical mesh models, the 8-rib wing model uses 287411 nodes and 139130 elements, the 9-rib wing model uses 296378 nodes and 143501 elements, and the 10-rib wing model uses 307227 nodes and 148944 elements.

Mesh convergence

To optimize the number of nodes and elements in the mathematical mesh model, mesh convergence was performed for the 9-rib wing model. The average mesh sizes were gradually reduced, and the mode shape frequencies were examined. It was assumed that further mesh size reduction would be meaningless in the region where the percentage change of the average relative change of the mode shape frequencies was below 0.3%; therefore, simulations continued using the mesh size in this region [27]. In modal analyses, where frequency values are very sensitive to changes in mesh size, using a relative change below 0.3% is important for the accuracy of the frequency value [1]. It was observed that the relative change was 0.157% when the average mesh size was reduced from 15 mm to 10 mm; therefore, an average mesh size of 15 mm was used for the simulation analyses. Table 2 shows the mesh convergence.

Table 2. Mesh Convergence.

Average mesh size, mm	Number of Elements	Number of Nodes	Frequency of Mod 1, Hz	Frequency of Mod 2, Hz	Frequency of Mod 3, Hz	Frequency of Mod 4, Hz	Relative Change, %

30	70852	147976	27.033	98.957	151.28	153.54	-
25	88549	185057	26.943	98.237	150.22	153.05	0.52
20	109620	226985	26.84	97.472	149.08	152.49	0.572
15	143501	296378	26.707	96.817	147.65	151.77	0.65
10	236983	859498	26.702	96.632	147.21	151.59	0.157

Physics of simulation

Six different simulations were performed on the created mathematical mesh models. In the first three simulations, modal analyses were performed on 8-rib, 9-rib, and 10-rib wing types, with the wing roots fixed and other regions left free. In the other three simulations, the 9-rib wing model was fixed at the wing root, and the degrees of freedom were restricted as if connected to the lateral strut under the fourth, fifth, and sixth ribs, counting from the wing root. Of the six degrees of freedom, two movements were restricted: vertical movement and movement away from or towards the root, in the region under a specific rib. All rotational movements and movements parallel to the longitudinal axis of the aircraft were left free in this region. To determine the frequency modes, three wing models differentiated according to the number of ribs and three simulation models of the 9-rib wing type with different positions under the wing were analyzed according to the position of the lateral strut. The models created based on the position of the lateral strut, according to which rib it is under from the wing root, were named 4-lateral strut, 5-lateral strut, and 6-lateral strut. In these analyses, the frequencies of the first four shape modes were determined, and the total deformation and maximum von-Misses stress values at these frequencies were also determined.

Results and Discussion

Frequency values were determined according to the first four mode shapes of the six analyses performed. The deformation shapes in the four natural vibration modes are shown in Figure 2. The dominant frequency ranges produced by the motor were named climbing frequency, cruise frequency, and descending frequency and marked as dangerous zones. Other regions were marked as safe zones. Figure 3 shows the analysis results plotted on the frequency regions separated into safe and dangerous zones according to motor frequencies.

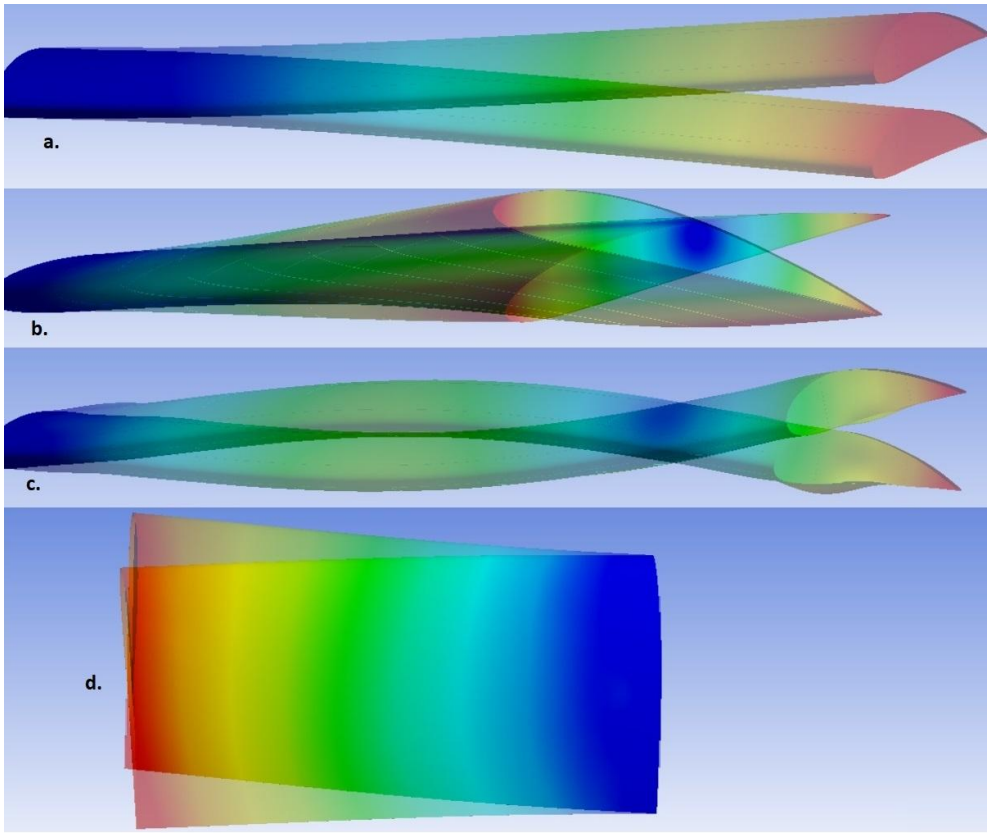


Figure 2. Deformation shapes of 9 rib wing according to mod shapes; a. Mod 1, b. Mod 2, c. Mod 3, d. Mod 4.

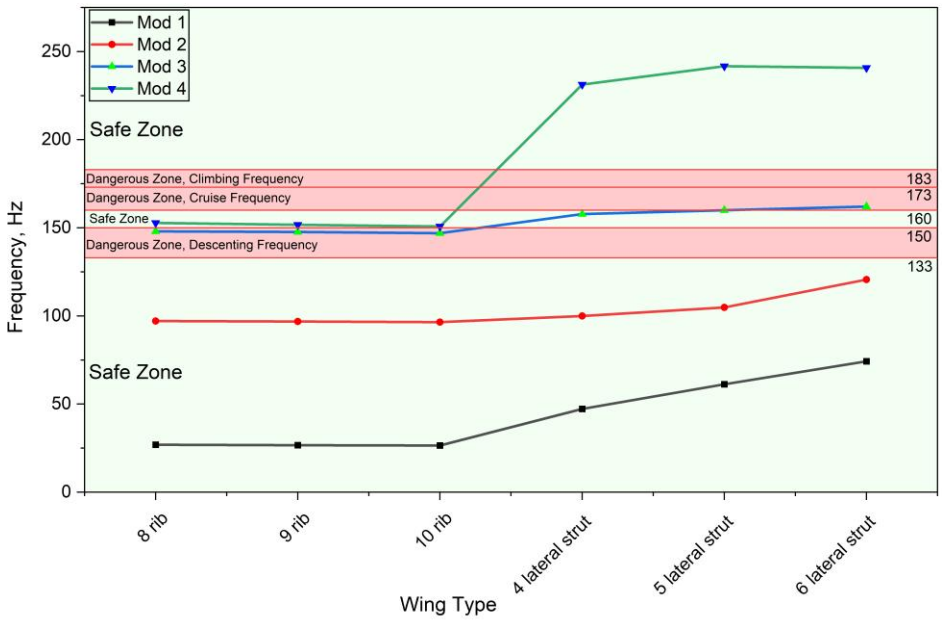


Figure 3. Natural frequencies of mod shapes according to wing type models.

Interpreting Figure 3, the natural frequencies of Modes 1 and 2 remain below the dominant engine frequencies, and when the wing is fixed with a lateral strut, the frequency values increase significantly. However, they are still below the dominant engine frequencies during descent. The natural frequency of Mode 3 coincides with the engine frequencies during descent in models without a lateral strut. When the lateral strut is attached below the 4th rib from the wing root, the natural frequency of this model falls between the level-flight engine speed and the descent engine speed and does not coincide with these frequencies. If the lateral strut is attached below the 5th or 6th rib, this natural frequency coincides with the engine's level-flight speed frequency. The natural frequencies of Mode 4 fall between the level-flight engine speed and the descent engine speed frequency in an 8-rib wing, while in wings with 9 or 10 ribs, they are at the limit of the engine's descent speed frequencies. When the wing is fixed with a lateral strut, the frequency value increases drastically, exceeding even the engine's climb rate frequency. Figure 4 shows the wingtip deformations according to the modes of the natural frequencies of different wing types.

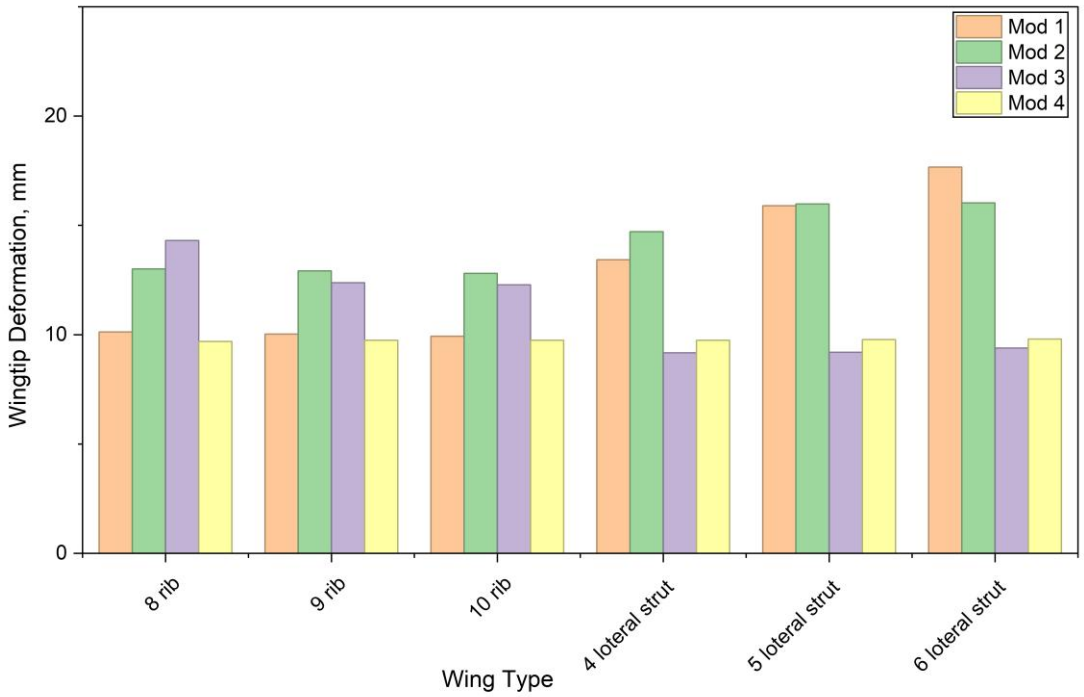


Figure 4. Wingtip deformations according to wing type.

Figure 5 shows the maximum von-Misses stress values generated in the wing structure according to the modes of the natural frequencies of the wing types.

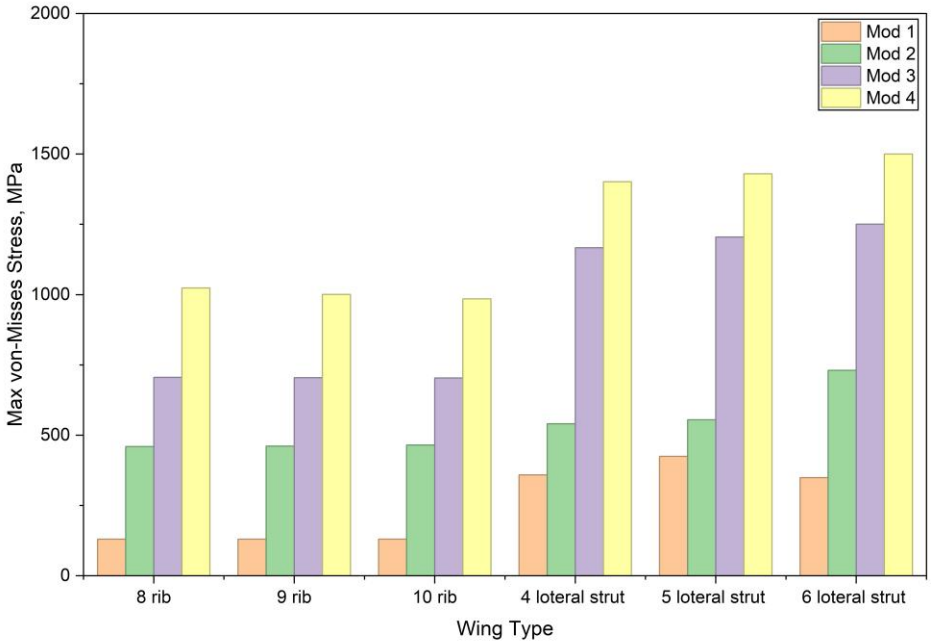


Figure 5. Maximum von-Misses stress value according to wing type.

Valuable validation of finite element method results based on quantitative comparison with literature

Frequency data obtained from modal analyses performed using the Finite Element Method were compared with analytical, experimental, and FEM data from existing studies to create a comparison table. This comparison table is shown in Table 3. According to Table 3, there is approximately a 2% - 12% difference in mode frequencies between this study and studies in literature. This difference is due to factors such as wingspan differences, differences in wing structural elements, and differences in the materials of the structural elements. However, this relative change value is not high and shows that the mode frequency values of this study are very close to reality. The limits of Physics of Simulation are very similar to the study by Ewins [11] and the fact that the results show a great similarity to the experimental results increases the reliability of the results of this study. In addition, the frequency changes in the study by Gürdal et al. [14] when a lateral strut-like structure is removed from the wing root are directly consistent with the results of this study. The results of other studies examined, particularly those using FEM analysis, are consistent with the results of this study [15,21,26]. Overall, the agreement between the results of this study and those of previous studies in the literature demonstrates that the mathematical network models developed in this study are quite sufficient and reliable for predicting the resonance occurring in the wings of a UAV or Ultra-Light aircraft under the influence of dominant vibrations generated by a Rotax-912 Boxer engine.

Table 3. Valuable Validation of Results.

Study	Structure Type	Mod	Mode Shape	Literature Frequency, Hz	Present Study, Hz	Relative Change, %
Ewins (2009)	Cantilever beam	Experimental/FEM	1	20–30	25–27	3–10%
Hodges & Pierce (2011)	Wing-like beam	Analytical	2	90–110	95–100	2–8%

Ouma et al. (2025)	Aircraft structure	FEM	2	100–130	96–120	5–12%
Wright & Cooper (2008)	Aircraft wing	Analytical	3	140–170	148–162	3–9%
Gürdal et al. (1999)	Composite wing	FEM	4	200–260	230–240	4–8%

Conclusions

The von-Misses stress values generated at the wing's natural frequencies are very high. Therefore, the dominant frequencies for the Rotax-912 engine at its typical operating speeds are 183-173 Hz for climbing, 173-160 Hz for cruising, and 150-133 Hz for descending, and these regions should not coincide with the wings' natural frequencies.

Changes in the number of ribs on a 2-meter single wingspan aircraft did not significantly alter its natural frequencies. Adding lateral struts under the wing increases the natural frequency values in all frequency modes. Especially the first two frequency modes remain well below the descending frequency, so there is no threat of resonance. However, caution should be exercised if the engine is to be run at idle speeds for extended periods during maintenance. This can be avoided by removing the wings. The clatter sound produced by the wings when the engine is started, especially in ultralight and light aircraft, is a familiar sound to pilots and is encountered in most aircraft. This is because at low speeds, the wing's first or second natural frequency mode coincides with the engine's low-speed frequency. Since the engine is usually not held at these speeds for very long, this does not pose a problem.

In aircraft with this short wingspan, the probability of the wing's third and fourth natural frequencies coinciding with the engine's dominant frequencies is very high. The change in the number of ribs on the wing did not bring the natural frequencies for the third and fourth frequency modes into the safe zone. However, adding a lateral strut to the wing significantly increased the frequency value of the fourth frequency mode, bringing it into the safe zone. The effect of the lateral strut is small for the third mode frequency value. Therefore, it is necessary to fit the third mode frequency value into the small safe range (160-150 Hz) between the engine's cruise and descending speeds. This was only achieved in the simulation with 4 lateral struts.

According to the change in rib number, the wingtip deformation did not change in the 1st, 2nd, and 4th frequency modes, while the 3rd frequency mode decreased as the rib number increased. Adding a lateral strut increased wingtip deformation in frequency modes 1 and 2 but decreased it in frequency mode 3. No change was observed in frequency mode 4. Advancing the lateral strut from the wing root to the wingtip increased wingtip deformation in frequency modes 1 and 2 but did not change it in frequency modes 3 and 4.

The highest von-Misses stress values were observed in frequency modes 3 and 4. Changes in the number of ribs on the wings did not change the von-Misses stress value. Adding a Canadian lateral strut increased von-Misses stress values in all frequency modes. When the lateral strut is advanced from the wing root to the wingtip, von-Misses stress values increase in all frequency modes.

Container lengths are an important parameter in determining the wingspan of ultralight and UAV aircraft transported to the customer in containers. The reason for using a 2m single wingspan aircraft as an example in this study is because container lengths are multiples of 2m. For ultralight aircraft with short wingspans, such as those designed with boxer engines like the Rotax-912, keeping the wings away from resonance zones caused by engine vibration is essential, especially considering past aircraft accidents.

References

1. Abrahamsson, T. J. S. & Kammer, D. C. Finite element model calibration using frequency responses with damping equalization. Mech. Syst. Signal Process. 62, 218–234 (2015). https://doi.org/10.1016/j.ymssp.2015.02.022

2. Adams, M. L. Rotating Machinery Vibration: From Analysis to Troubleshooting, 2nd ed. CRC Press (2010).

3. Bisplinghoff, R. L., Ashley, H. & Halfman, R. L. Aeroelasticity. Courier Corporation (2013).

4. Burdzik, R. Research on the influence of engine rotational speed to the vibration penetration into the driver via feet—multidimensional analysis. J. Vibroengineering 15, 2114–2123 (2013).

5. Civil Aeronautics Board. Aircraft Accident Report—Northwest Airlines Flight 710, Lockheed L-188 Electra (1961). https://www.faa.gov/sites/faa.gov/files/2022-11/CAB%20Aircraft%20Accident%20Report%20-%20Northwest%20Airlines%20Lockheed%20Electra%20-%20N121US.pdf

6. Civil Aeronautics Board. Aircraft Accident Report—Braniff Airways Flight 542 (1962). https://rosap.ntl.bts.gov/view/dot/33609

7. Criollo, L. et al. Modal and random vibration analysis for structural design of aircraft external stores. Aviation 29, 137–149 (2025). https://doi.org/10.3846/aviation.2025.24456

8. Demircali, A. A. & Uvet, H. Mini glider design and implementation with wing-folding mechanism. Appl. Sci. 8, 1541 (2018). https://doi.org/10.3390/app8091541

9. Den Hartog, J. P. Mechanical Vibrations, 4th ed. Courier Corporation (1985).

10. Evran, S. Investigation of the effects of aspect ratio and taper ratio on aircraft wing vibration. J. Aviat. 4, 140–146 (2020). https://doi.org/10.30518/jav.778273

11. Ewins, D. J. Modal Testing: Theory, Practice and Application, 2nd ed. Wiley (2009).

12. Gennaretti, M. Fundamentals of Aeroelasticity. Springer Nature (2024).

13. Goliasz, T. & Czarnigowski, J. Analysis of middle range frequency vibration of aircraft reciprocating engine. J. KONES 24, 151–158 (2017).

14. Gürdal, Z., Haftka, R. T. & Hajela, P. Design and Optimization of Laminated Composite Materials. Wiley (1999).

15. Hodges, D. H. & Pierce, G. A. Introduction to Structural Dynamics and Aeroelasticity, 2nd ed. Cambridge Univ. Press (2011). https://doi.org/10.1017/CBO9780511997112

16. Li, K. et al. Multiscale aeroelastic optimization method for wing structure and material. Aerospace 10, 866 (2023). https://doi.org/10.3390/aerospace10100866

17. Lin, Z., Chen, Y. & Wu, M. Research on the vibration isolation performance of low-frequency hydraulic engine mount. Int. J. Veh. Noise Vib. 19, 78–97 (2023). https://doi.org/10.1504/IJVNV.2023.130250

18. Liu, L. & Tian, B. Vibration suppression of flexible aircraft using ADRC. Sensors 22, 6207 (2022). https://doi.org/10.3390/s22166207

19. National Transportation Safety Board. Preliminary Report—UPS Airlines Flight 2976 (2025). https://www.ntsb.gov/investigations/Documents/Preliminary%20Report%20DCA26MA024.pdf

20. Otkur, M. Altitude performance and fuel consumption modelling of Rotax 912. J. Adv. Res. Appl. Sci. Eng. Technol. 23, 18–25 (2021). https://doi.org/10.37934/araset.23.1.1825

21. Ouma, M. O., Deng, H. & Xue, C. Optimization of aircraft engine mount system for vibration isolation. Aerospace 13, 48 (2025). https://doi.org/10.3390/aerospace13010048

22. Qaumi, T. & Hashemi, S. M. Experimental and numerical modal analysis of composite rocket structure. Aerospace 10, 867 (2023). https://doi.org/10.3390/aerospace10100867

23. Randall, R. B. Vibration-Based Condition Monitoring: Industrial, Automotive and Aerospace Applications, 2nd ed. Wiley (2021).

24. Sarı, B., Lıchaeı, M. K. & Yıldırım, S. Free vibration analysis of tapered composite aircraft wing via finite element method. Cukurova Univ. J. Fac. Eng. 37, 741–752 (2022). https://doi.org/10.21605/cukurovaumfd.1190386

25. Takahashi, N., Nakagawa, S. & Mikami, M. Investigation of combustion-induced vibration sources using wavelet analysis. Meas. Energy 5, 100037 (2025). https://doi.org/10.1016/j.meaene.2025.100037

26. Wright, J. R. & Cooper, J. E. Introduction to Aircraft Aeroelasticity and Loads, Vol. 18. Wiley (2008).

27. Xie, J. et al. Influence of finite element meshing accuracy on modal analysis. Pol. Marit. Res. 25(S3), 147–153 (2018). https://doi.org/10.2478/pomr-2018-0122

Funding: No funding.